# Habitual higher order aberrations affect Landolt but not Vernier acuity

**Jenny L. Reiniger** Department of Ophthalmology, University of Bonn, Germany

**Anne C. Lobecke** Department of Neurobiology, University of Bielefeld, Germany

**Ramkumar Sabesan** Department of Ophthalmology, University of Washington, Seattle, WA, USA

**Michael Bach** Eye Center, Medical Center—University of Freiburg, Faculty of Medicine, University of Freiburg, Germany

**Frenne Verbakel** University Eye Clinic Maastricht, The Netherlands

**John de Brabander** University Eye Clinic Maastricht, The Netherlands

**Frank G. Holz** Department of Ophthalmology, University of Bonn, Germany

**Tos T. J. M. Berendschot** University Eye Clinic Maastricht, The Netherlands

**Wolf M. Harmening** Department of Ophthalmology, University of Bonn, Germany

**To assess whether the eye's optical imperfections are relevant for hyperacute vision, we measured ocular wave aberrations, visual hyperacuity, and acuity thresholds in 31 eyes of young adults. Although there was a significant positive correlation between the subjects' performance in Vernier- and Landolt-optotype acuity tasks, we found clear differences in how far both acuity measures correlate with the eyes' optics. Landolt acuity thresholds were significantly better in eyes with low higher order aberrations and high visual Strehl ratios ($r^2 = 0.22$, $p = 0.009$), and significantly positively correlated with axial length ($r^2 = 0.15$, $p = 0.03$). A retinal image quality metric, calculated as two-dimensional correlation between perfect and actual retinal image, was also correlated with Landolt acuity thresholds ($r^2 = 0.27$, $p = 0.003$). No such correlations were found with Vernier acuity performance ($r^2 < 0.03$, $p > 0.3$). Based on these results, hyperacuity thresholds are, contrary to resolution acuity, not affected by higher order aberrations of the eye.**

## Introduction

The relationship between optical quality of the eye and its primary function, seeing, is a well-studied field. Typically, a special emphasis is given to measurements of visual acuity, the ability to discriminate small visual optotypes, because of the natural simplicity of how such measurements can be performed, their applicability for clinical assessment of visual function, and their profound meaning in real-life situations. On the other hand, in everyday vision tasks, seeing is comprised of more than reading letters, and it seems that our eyes and brain have evolved to make use of even the tiniest spatial information available. This is

Citation: Reiniger, J. L., Lobecke, A. C., Sabesan, R., Bach, M., Verbakel, F., de Brabander, J., Holz, F. G., Berendschot, T. T. J. M., & Harmening, W. M. (2019). Habitual higher order aberrations affect Landolt but not Vernier acuity. *Journal of Vision, 19*(5):11, 1–15, https://doi.org/10.1167/19.5.11.

https://doi.org/10.1167/19.5.11 Received July 13, 2018; published May 17, 2019 ISSN 1534-7362 

exemplified by our ability to detect the offset in a pair of lines or dots to a much finer degree than we are able to read. Psychophysical thresholds derived from Vernier and similar positional discrimination tasks are usually only a fraction of the eye's resolving power, and are well below the two-point sampling capacity of the retinal photoreceptor mosaic (Curcio, Sloan, Kalina, & Hendrickson, 1990; Hering, 1899; Hirsch & Curcio, 1989; Strasburger, Huber, & Rose, 2018). This is why the perceptual performance in these tasks was termed hyperacuity (Westheimer, 1975).

Since its first encounter (Wülfing, 1892), the interrelation between stimulus and perceptual characteristics in hyperacuity tasks have been described in diverse approaches. Besides other parameters, the dependencies of spatial configuration (Westheimer & McKee, 1977), luminance (Bradley & Skottun, 1987), contrast (Wehrhahn & Westheimer, 1990), motion (Westheimer & McKee, 1975), spatial frequency (Whitaker & MacVeigh, 1991), and orientation (Westheimer, Shimamura, & McKee, 1976) were studied before. Hyperacuity is subject to short-term task learning (Mckee & Westheimer, 1978), and has become a model paradigm for studies of long-term perceptual learning (Fahle, 1993). Consequentially, physiological and computational models of the mechanisms behind hyperacuity have been developed (Findlay, 1973; Geisler, 1984; Jiang et al., 2017), identifying Vernier acuity not being some miraculous singularity, but an intrinsic property of the neural networks underlying spatial vision (Westheimer, 2009). This is further illustrated by the fact that Vernier acuity is also a hyperacuity phenomenon in other species, such as monkeys (Kiorpes, Kiper, & Movshon, 1993), cats (Murphy & Mitchell, 1991), rats (Seymoure & Juraska, 1997), and birds (Harmening, Göbbels, & Wagner, 2007).

By artificial large-scale deterioration of the retinal image like blurring one's vision with trial lenses or semitranslucent screens, it was demonstrated that two-point acuity and Vernier acuity vary markedly as a function of blur (Bedell, Patel, & Chung, 1999; Krauskopf & Farell, 1991; Levi & Klein, 1990). However, the impairment of Vernier thresholds by retinal image degradation is highly dependent on the chosen stimulus parameters (e.g., gap size) (Williams, Enoch, & Essock, 1984). Different neurological visual disorders, like strabismic or anisometropic amblyopia, were shown to have distinct relations to visual acuity and grating resolution, differing from subjects with normal vision, thus Vernier acuity was established to research the etiology of amblyopia (Hou, Good, & Norcia, 2018; Levi & Klein, 1982). Comparably, less is known about how small-scale image degradation by the habitual optics of the eye, especially higher order aberrations—imperfections that cannot be corrected with glasses or contact lenses—interact with acuity thresholds. For conventional resolution tasks, the relationship between the habitual higher order ocular aberrations and their effect on perceptual performance cannot be readily inferred by conclusions drawn from artificially altered retinal image quality. For example, while an adaptive optics correction of the higher-order ocular aberrations can improve visual acuity to degrees that are in agreement with the eye's optical modulation transfer function (Yoon & Williams, 2002), the question of whether visual acuity in subjects with less higher-order aberrations is better than in those with more aberrations was not clearly answered for a population with normal and excellent visual acuities (Villegas, Alcon, & Artal, 2008).

We here ask how far hyperacuity thresholds depend on the eye's habitual optical quality in healthy subjects. Because of the surprisingly limited number of studies relating normal visual acuity to habitual ocular aberrations, and to address possible differences and relations across the two acuity measurements, we also assessed Landolt acuity in the same subjects.

## Material and methods

### Subjects

Acuity thresholds and optical measurements were assessed in both eyes of 32 young adults. Subjects were student volunteers at the RWTH Aachen chosen without prior visual screening and two of the authors (ACL, WMH). One subject was excluded from further analysis because of exceptionally high between-eyes threshold differences. The remaining 31 subjects were aged 22–36 (mean ± standard deviation: 27 ± 3 years), 12 subjects were female. Subjects participated in two separate experiments (acuity and optical measurements) carried out on two different days. During acuity assessment, ametropic participants wore their habitual correction (contact lenses, $n = 8$; spectacles, $n = 8$), emmetropic subjects wore no correction ($n = 15$). For acuity-optics correlation analyses, results from only the right eyes were used (Supplementary Table S1). Written informed consent was obtained from all participants after the experiment procedures and possible risks had been explained verbally. The study was performed in compliance with the tenets of the Declaration of Helsinki.

### Acuity measurements

Acuity thresholds (Landolt-optotype acuity and Vernier acuity, respectively) were obtained in a

psychophysical experiment. Subjects were seated 13 m in front of an LCD panel (Belinea, Germany; angular pixel pitch ~4.5 arcsec), which delivered visual stimuli generated by the "Freiburg Visual Acuity and Contrast Test" (FrACT, version 3.5, https://michaelbach.de/fract/), a customizable acuity testing software. Acuity thresholds were obtained both binocularly and monocularly, with the fellow eye occluded by a translucent sheet in monocular runs (Figure 1A). Visual stimuli were high-contrast, dark optotypes presented on a bright background (background luminance: 300 cd/m$^2$, Michelson contrast: 0.99). Optotypes were either Landolt Cs of variable size or a pair of horizontally displaced lines with a Gaussian luminance profile of fixed size (physical dimensions in degree of visual angle, total stimulus height: 0.5°, line sigma: 0.5 arcmin, gap height: 0.2 arcmin). Psychophysical procedures employed by the FrACT have been described in detail elsewhere (Bach, 1996, 2007). Briefly, a forced-choice, adaptive staircase with self-paced trial progress was used. The subject's task was to discriminate between eight possible directions of gap openings in the Landolt C, or between one of two offset directions in the Vernier lines, respectively. Following the applied best parameter estimation by sequential testing procedure (Lieberman & Pentland, 1982), stimulus intensities at each trial equaled the current threshold estimate (Figure 1B). A motivating high intensity trial was introduced every sixth trial. The staircase terminated after 24 trials in Landolt acuity tests and after 42 trials in Vernier acuity tests, and the next estimate after recording the last response was taken as the threshold outcome. Subjects indicated their response by pressing the corresponding key on a computer keyboard. Calculated as the mean of 6–8 consecutive runs, acuity thresholds are expressed in logMAR, the logarithmic minimum angle of resolution in minutes of arc of visual angle. Pupil size was measured concurrently during all behavioral experimental trials by video pupillometry. The mean value of a stable sequence of pupil diameter across 5 s at the end of each behavioral run is reported here and was used for further analysis (Supplementary Table S1).

## Optical measurements and data analysis

Optical quality of the subjects' eyes was assessed by measuring the ocular wavefront aberrations using a near-infrared (785 nm) thin beam principle of optical ray tracing across a 5-mm pupil (iTrace, Tracey Technologies, Houston, TX). Measurements were carried out at natural viewing conditions, i.e., subjects did not wear their habitual correction, and no accommodative block, pupil dilation, or corneal lubrication was administered. The experimental room

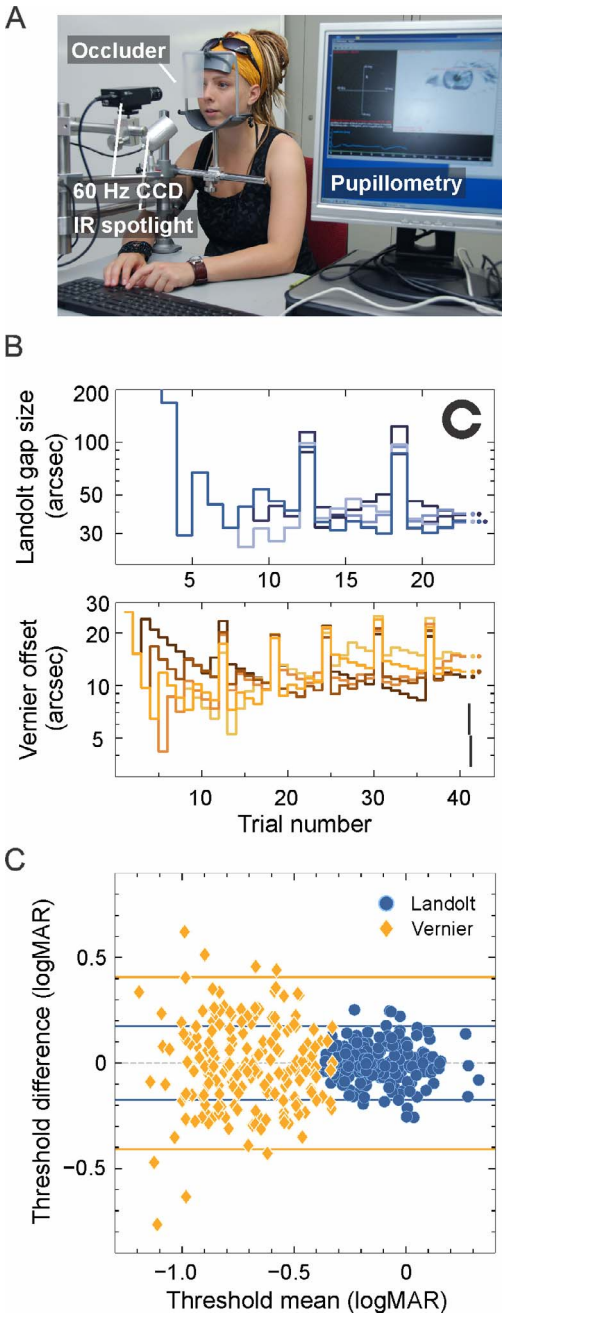


Figure 1. Behavioral testing. (A) The observer's viewing stage during psychophysical measurements. A head and chin rest provided constant viewing distance (13 m), and stable eye positioning for custom video pupillometry. (B) Example staircases for Landolt (top) and Vernier (bottom) acuity estimation. Five repeated runs are shown; the final threshold estimation is given by the filled circles. Note the motivating "bonus" trials every sixth trial. Example stimuli for Landolt/Vernier acuity testing are shown in the upper and lower right corner, respectively. (C) Bland-Altman analysis, plotting the difference between each pair of two consecutive monocular threshold measurements against their mean value in logMAR. Horizontal lines mark the 95% interval of threshold differences. Blue circles are results from Landolt acuity measurements, yellow diamonds are Vernier acuity results.

was darkened to allow maximum natural pupil sizes. Subjects were prompted to blink their eyes normally. The mean of three consecutive measurements was used to express wavefront errors as the Zernike polynomial expansion up to the eighth order (Supplementary Table S1). Axial length (AL) was determined by optical low coherence reflectometry with a Lenstar LS 900 (Haag-Streit, Koeniz, Switzerland). To report optical quality of the subjects' eyes during behavioral testing, wavefront errors that were recorded at 5 mm pupil diameter had to be recalculated and scaled to the actual pupil diameter present during behavioral testing. A set of recursive conversion equations was used for the rescaling of individual Zernike terms (calculations based on equations presented in Schwiegerling, 2002, using a correction term shown in Visser et al., 2011). The point-spread function (PSF) of each eye was calculated (Maeda, 2008) and further used to calculate theoretical retinal image quality by convolution of computer generated vector graphics. Because accommodation was not controlled for during acuity and optical measurements and the exact refractive state was unknown during behavioral testing, a through-focus analysis was carried out: for each eye, a combined defocus/astigmatism term was computationally found that optimized retinal image quality (defined as image correlation maximum between measured and ideal PSF-convoluted images; see next paragraph). Because lower order aberrations (LOA) in half of the subjects were corrected by their individual habitual correction (contact or spectacle lenses), we also calculated the theoretical residual lower order aberrations as the difference between the power vectors (Thibos, Wheeler, & Horner, 1997) of measured and corrected LOA (defocus and astigmatism). Spectacle prescriptions were corrected for a standard cornea vertex distance of 12 mm.

To report wavefront aberrations independent of the individual pupil diameter during acuity experiments, root mean square error was normalized by the pupil area and converted to an ophthalmic prescription, expressed as the equivalent defocus in diopters (Thibos, Hong, Bradley, & Cheng, 2002). To quantify retinal image quality, three different metrics were calculated for each eye. The Strehl ratio of an optical system is defined as the ratio between the peak intensity of the PSFs in the actual system versus one from a diffraction-limited system. The visual Strehl ratio (VSX) additionally incorporates a standardized neural weighting function (Thibos, Hong, Bradley, & Applegate, 2004) and has been shown to have a stronger correlation with visual performance (Marsack, Thibos, & Applegate, 2004). Finally, an image convolution-based method described by Watson and Ahumada (2008) and modified by Zheleznyak, Sabesan, Oh, MacRae, and Yoon (2013) was used. Briefly, the individual PSF's were calculated for polychromatic white light (405–695 nm wavelength, weighted by the photopic spectral sensitivity function $V_\lambda$) (Ravikumar, Thibos, & Bradley, 2008). Computer-generated bitmaps of the retinal stimulus at threshold (size = mean threshold of all eyes) were then convolved with both, a diffraction limited PSF and the actual PSF of the individual eye. The two-dimensional image correlation coefficient (MATLAB, MathWorks, Natick, MA; 2-D correlation coefficient *corr2*) calculated between both images is then used as the retinal image quality metric. The metric's values range between 0 and 1, where 1 would imply that the individual PSF's retinal stimulus image is identical to the diffraction limited one (Watson & Ahumada, 2008; Zheleznyak et al., 2013).

Because many of the optical parameters and image quality metrics found here were not normally distributed, we used Spearman's rank correlation for evaluating those data. For comparing the normally distributed acuity threshold of Landolt and Vernier measurements, Pearson's correlation was calculated.

# Results

## Landolt and Vernier acuity thresholds

We measured Vernier and visual acuity with the "Freiburg visual acuity and contrast test" (FrACT; see Acuity measurements), a test software that has so far been applied to measure normal acuity and contrast sensitivity (Bühren, Terzi, Bach, Wesemann, & Kohnen, 2006; Rocha, Vabre, Chateau, & Krueger, 2010), but not hyperacuity thresholds. Thus, we first wished to confirm the validity of the methods applied here and procedures to correctly identify the subjects' Vernier acuity, by comparing our results with the literature on Vernier acuity thresholds in healthy subjects.

Across all tested eyes, we found thresholds to be normally distributed ranging from −1.06 to −0.36 logMAR (equaling 5.2 to 25.9 seconds of arc), with an overall mean threshold of −0.7 ± 0.2 logMAR (11.5 ± 3.5 arcsec) (Figure 2A). Landolt acuity values were normally distributed as well. With a mean Landolt acuity of −0.1 ± 0.1 logMAR (45.1 ± 7.0 arcsec) in our experiments, the mean hyperacuity ratio (Landolt acuity/Vernier acuity threshold) was 4.1, although the individual per eye ratios differed substantially (range: 1.4–10.6). These findings match reports where Vernier acuity tests were performed with untrained subjects (Abbud & Cruz, 2002). By combining two individual consecutive measurements to form a test/retest pair, a Bland-Altman plot was constructed (Figure 1C). Note that 95% of all test/retest differences lay within a range of about ±0.41 logMAR for Vernier thresholds, whereas the differences between Landolt acuity

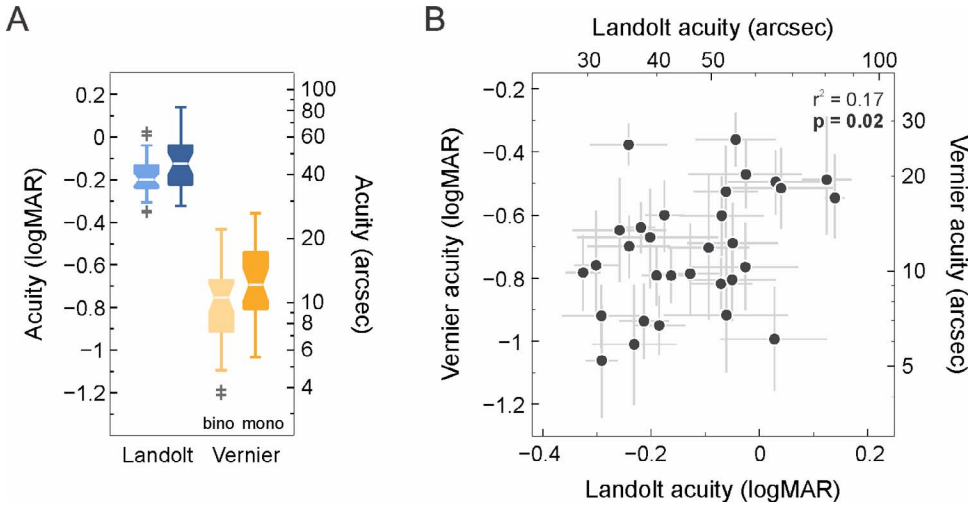


Figure 2. Psychophysical acuity thresholds. (A) Binocular ("bino," light) and monocular ("mono," dark) thresholds for Landolt and Vernier acuity for all 31 subjects are shown as boxplots. Landolt and Vernier acuity values are plotted in blue and yellow, respectively. Horizontal lines signify medians, the edges of the box are the first and third quartile [interquartile range (IQR)], notches display the 95% confidence interval of the median and whiskers extend to the most extreme data points without outliers (>1.5 IQR), which are shown with individual cross markers. Monocular and binocular thresholds for Landolt and Vernier acuity differ significantly (*t* test, $p \ll 0.001$). (B) Vernier acuity thresholds plotted against Landolt acuity thresholds of all right eyes. The gray error bars represent the standard deviations of threshold estimates between the consecutive measurements. The two metrics are significantly positively correlated ($r^2 = 0.17$, $p = 0.02$).

thresholds were in the range of about ±0.18 logMAR. The mean coefficients of variance (CVs; i.e., standard deviation divided by mean) of our Vernier measurements were 0.30 and 0.29 (binocular and monocular, respectively). This is contrasted by mean CVs of 0.1 and 0.15 in Landolt acuity thresholds. Expressed differently, the mean standard error for Vernier thresholds was between 0.53 and 0.67 arcsec, and 0.73–1.3 arcsec in Landolt tests. These findings match earlier results (Lindblom & Westheimer, 1989), and confirm that measures of Vernier acuity are prone to relatively large intertest variability (Abbud & Cruz, 2002). Vernier acuity is subject to binocular summation, i.e., thresholds measured with two eyes are usually lower (better) than those measured with one eye alone. We find a mean summation ratio of 1.35 (range: 0.6–3.6). These results are in agreement with earlier findings performed at similar stimulus configuration and contrast (Banton & Levi, 1991; Lindblom & Westheimer, 1989). In conclusion, our behavioral results generally paralleled earlier results, and we were therefore confident that the here applied stimuli and methods provide sufficient fidelity to measure Vernier acuity with the FrACT in untrained subjects.

The correlation between Landolt and Vernier acuity thresholds across eyes (Figure 2B) was significantly positive ($p = 0.02$). That is, subjects that had good performance in the Landolt test tended to have lower thresholds in the Vernier task as well. As one example, the subject with the lowest mean Vernier acuity threshold (−1.06 logMAR) had a mean Landolt acuity threshold of −0.29, among the lowest within the study. Equally, the subject with one of the highest mean Landolt acuity thresholds (0.12 logMAR) also had one of the highest Vernier acuity thresholds (−0.49 logMAR). However, overall predictive power of the correlation was relatively weak ($r^2 = 0.17$). The linear fit to the threshold data expressed in logMAR had a slope of 0.68, indicating an exponential relation between Landolt and Vernier acuity thresholds on a linear scale.

## Ocular biometry and optical quality

Ocular biometry of all eyes was assessed by pupil diameter measurement during psychophysical testing and by axial length measurements during optical testing. The pupil size varied between 3.1 and 4.8 mm (mean ± SD: 3.8 ± 0.46 mm) during Landolt and 3.1–4.9 mm (mean ± SD: 3.8 ± 0.45 mm) during Vernier acuity testing (Figure 3A). Pupil sizes during both acuity experiments were highly correlated ($r^2 = 0.86$, $p \ll 0.001$), with an average deviation between pupil diameters of 0.14 mm (±0.11 mm). During aberration measurements, all pupil diameters were under natural conditions, but larger than 5 mm, a prerequisite for wavefront aberration measurements. Axial lengths were between 22.3 mm and 27.2 mm (mean ± SD: 24.3 ± 1.2 mm; Figure 3B) and were strongly correlated with the individual eyes' lower order aberrations ($r^2 = 0.56$, $p \ll 0.001$).

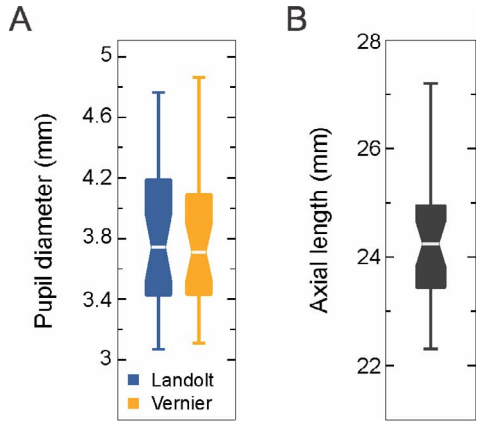


Figure 3. Ocular biometry. (A) Pupil diameter for Landolt (blue) and Vernier (yellow) acuity measurements determined by video pupillometry during behavioral testing. Wavefront aberrations were measured for a 5 mm pupil size and Zernike coefficients were recalculated for analysis according to the pupil sizes measured during vision testing. (B) Axial length determined by low coherence reflectometry. Boxplot conventions as in Figure 2.

Optical quality was assessed by measuring the ocular wave aberrations under natural viewing conditions and with natural pupils. Reported wavefront errors are given for a 5 mm pupil diameter. Wave aberrations of all eyes were expressed as a set of Zernike coefficients up to the eighth order (Figure 4A and B). Since we aimed to measure visual performance under natural viewing conditions, ametropic subjects wore their habitual correction devices (spectacles or contact lenses) during acuity tests. For these subjects, refractive defocus correction was between 0 and −8.0 D; however, 75% of the eyes had a prescribed defocus of −3.0 D or less and three-fourths of the remaining subjects with higher myopia wore contact lenses for correction. Prescribed astigmatic correction was −0.75 D or less in 90% of all eyes, with three of the subjects needing higher astigmatic corrections of −1.5, −1.75, and −2.25 D, respectively. The resulting residual defocus values (difference between objectively measured and corrected LOA) were on average −0.12 D (between −1.63 and 2.35 D). The calculated mean residual absolute astigmatism was 0.44 D (between 0.02 and 1.5 D), with 66% of all eyes having a residual astigmatism below 0.5 D (Figure 4A; habitual correction).

Higher order aberrations (HOA) had an average root mean square (RMS) of 0.2 ± 0.06 μm and ranged between 0.07 and 0.34 μm. Individual Zernike coefficients of coma, trefoil (averaged horizontal and vertical) and spherical aberration ranged from 0.02 μm to 0.26 μm, 0.02–0.19 μm, and 0.07–0.19 μm, respectively. Due to the smaller pupil sizes measured during behavioral testing, the impact of ocular aberrations was lower in those conditions. Zernike coefficients were thus recalculated to scale to the individual pupil sizes present during behavioral tests. As a metric of optical quality which factors out the different pupil sizes, we calculated the HOA equivalent defocus (Figure 4C). The mean equivalent defocus for HOA measured at 5 mm pupils was 0.23 D ± 0.07 D (range: 0.07–0.38 D). Average HOA equivalent defocus was similar during Vernier and Landolt acuity measurement (because of

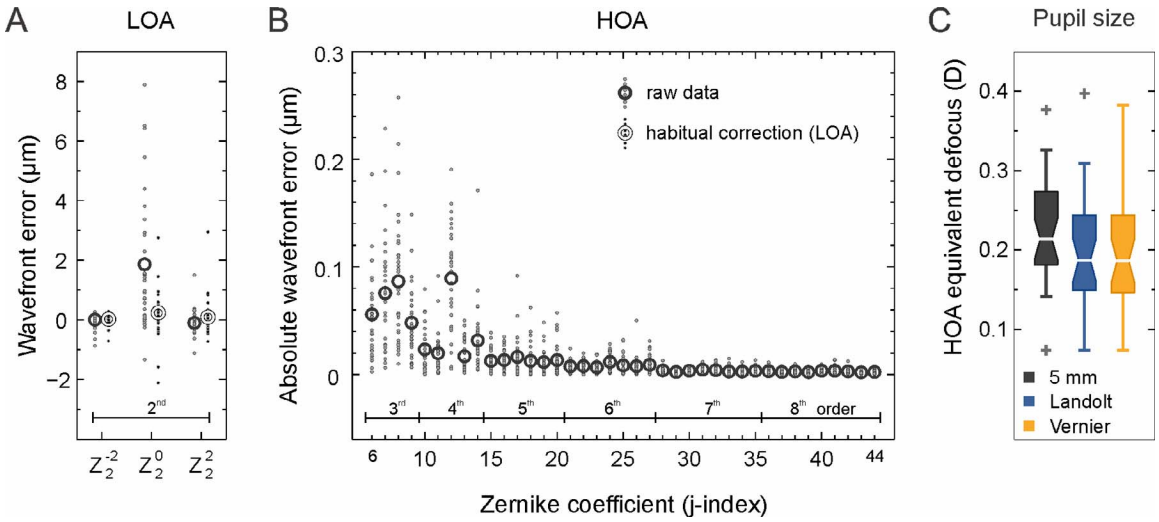


Figure 4. Ocular wavefront errors. (A) Lower order wavefront aberrations (LOA) of all eyes (5 mm pupil size). Small dots are individual eyes, circle markers are average values across eyes. Dark circles are raw data; bright circles are residual errors after correcting for habitual correction devices, worn by some subjects. (B) Absolute higher order aberrations (HOA) expressed in μm of all eyes (5 mm pupil size). Small dots are individual eyes; circle markers are average values across eyes. (C) Equivalent defocus values for HOA (Zernike order 3–8), calculated by normalizing the HOA by the individual pupil area during Landolt/Vernier acuity experiments, ($n$ = 31). Boxplot conventions as in Figure 2.

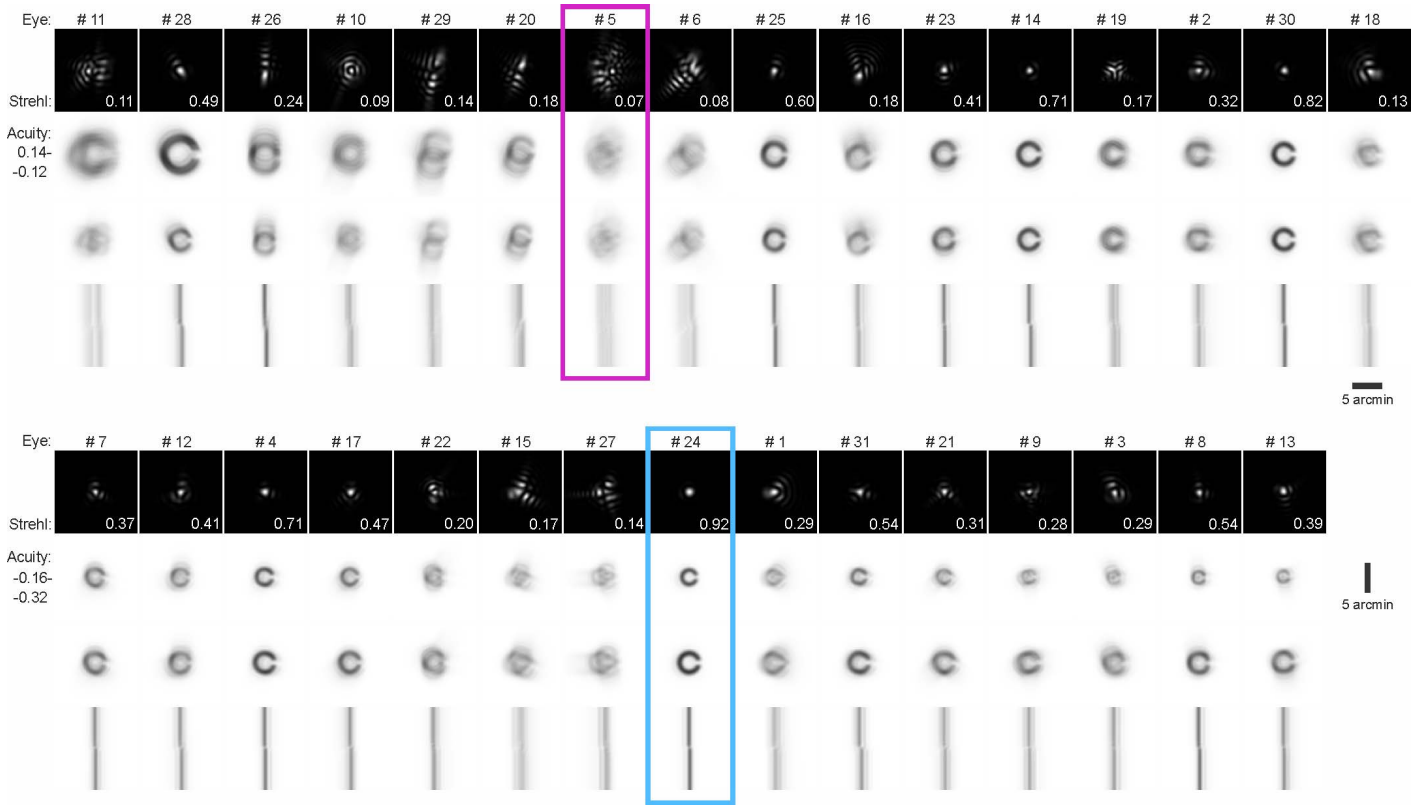


Figure 5. Retinal image quality. Qualitative representation of individual wavefront aberrations and their impact on the retinal image. The data of 31 tested eyes are shown in two rows, consisting of four different analyses ordered by the individual Landolt acuity thresholds (in logMAR), from worst (top left) to best (bottom right). Point spread functions (PSF) are shown in the first row (theoretical distribution of monochromatic light, 555 nm, normalized to span 0 to 1 for better visibility). Strehl ratio values are shown in the lower right corner of the PSF images. Rows two to four show a convolution of the individual PSF with: Landolt stimuli scaled to individual threshold size (row 2), Landolt stimuli at a fixed size (row 3), and the center part of the Vernier stimulus scaled to individual threshold size (row 4). The two subjects with highest and the lowest Strehl ratio are highlighted in light blue and magenta, respectively (compare Figure 6, 7). The edge length of PSF images is 10 arcmin, the scale bar for all stimulus images is 5 arcmin.

the similar pupil sizes, compare Figure 3A), with mean values of 0.20 D ± 0.07 D and 0.19 D ± 0.07 D during Landolt and Vernier acuity testing, respectively. The range of HOA equivalent defocus values was also similar for Landolt (0.07–0.40 D) and Vernier (0.07–0.38 D) acuity measurements.

## Retinal image quality metrics and correlations

To assess retinal image quality, the polychromatic PSF was calculated for each eye and convolved with computer generated bitmaps of the optotypes used in the acuity experiments. Figure 5 arranges the PSFs of all 31 eyes ordered by their visual acuity (Landolt C), suggesting qualitatively that eyes with "better" PSF's have higher visual acuities. Accordingly, the Strehl ratio values (first row in Figure 5), were negatively correlated with Landolt acuity thresholds ($r^2 = 0.18$, $p = 0.016$), implying that eyes with higher Strehl ratios tended to have better visual acuity thresholds. When the eye's individual PSF was convolved with a computer-generated stimulus image at a fixed size (–0.12 logMAR, average threshold), retinal image quality seemed to qualitatively improve with increasing visual acuity (third row in Figure 5). This is similar for Vernier acuity stimuli, although Strehl ratios were not significantly correlated with Vernier thresholds ($r^2 = 0.02$, $p = 0.51$). In general, we observe a broad distribution of visual acuity thresholds for similar amounts of aberration.

Since the optics of an individual eye are an essential factor for the formation of the retinal image, we analyzed optical quality as well as optical biometry as factors potentially influencing acuity thresholds. We find a weak positive correlation between axial length (AL) and Landolt acuity ($r^2 = 0.15$, $p = 0.03$) but no significant correlation between AL and Vernier acuity thresholds ($r^2 = 0.01$, $p = 0.62$) (Figure 6). There was no significant correlation between the amount of HOA RMS (μm) at a 5 mm pupil and AL ($r^2 = 0.01$, $p = 0.55$). However, there was a weak positive correlation

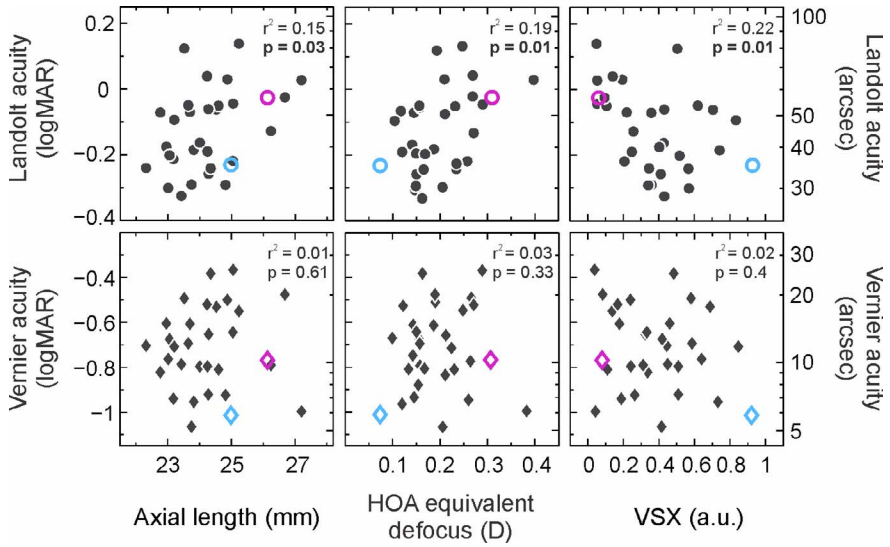


Figure 6. Correlation of behavioral and optical parameters. Landolt and Vernier acuity thresholds are plotted against optical parameters: axial length, HOA equivalent defocus and visual Strehl ratio (VSX) ($n = 31$). Coefficients of determination $r^2$ and probability values p (Spearman's rank correlation) are shown in the upper right corner of each plot. Data points of the two subjects with the highest and lowest Strehl ratio are plotted in light blue and magenta, respectively (compare Figure 5).

between HOA RMS and Landolt acuity thresholds ($r^2 = 0.15$, $p = 0.03$), whereas no correlation was found between HOA RMS and Vernier acuity thresholds ($r^2 = 0.02$, $p = 0.46$). Zernike coefficients of second (residual LOA) and third order (spherical aberration, coma, and trefoil) were examined separately. Neither Landolt nor Vernier acuity correlated with the total residual LOA. Coma was positively correlated with Landolt acuity ($r^2 = 0.22$, $p = 0.008$), but not significantly correlated with Vernier acuity ($r^2 = 0.002$, $p = 0.81$). No correlation with either of the acuities could be found for spherical aberration or trefoil. We also calculated the HOA equivalent defocus for factoring out the individual pupil sizes during experiments (Figure 6). Landolt acuity thresholds showed a significantly positive correlation with the HOA equivalent defocus ($r^2 = 0.19$, $p = 0.014$), but no correlation was found for Vernier acuity thresholds ($r^2 = 0.03$, $p = 0.33$).

It has to be noted that metrics of optical quality in the pupil plane, such as HOA equivalent defocus, may be limited to describe subjective image quality and visibility, because further downstream retinal and neural factors play a key role in image processing steps and the final perceptual decision. We included VSX and a two-dimensional image correlation coefficient in our analysis as two additional metrics to meet this concern. Landolt acuity thresholds were negatively correlated with VSX ($r^2 = 0.22$, $p = 0.009$), i.e., eyes with higher VSX values also had better visual acuity thresholds. Vernier acuity thresholds were not significantly correlated with VSX ($r^2 = 0.02$, $p = 0.4$). The image correlation metric (Figure 7A) also revealed a difference in how the retinal images correlate with Landolt and Vernier acuity thresholds, respectively. Similar to most of the other analyzed metrics, Landolt acuity was significantly correlated with the image correlation coefficients ($r^2 = 0.27$, $p = 0.003$). Vernier acuity thresholds, on the other hand, did not correlate with the image correlation coefficients ($r^2 = 0.002$, $p = 0.8$). As an example, the two subjects with the highest and the lowest Strehl ratio (plotted in light blue and magenta, respectively) populate different parts of the spectrum of exhibited acuity thresholds. Landolt acuity thresholds of those subjects were in the upper versus lower half of the spectrum and for Vernier acuity, both thresholds were in the upper half of the acuity spectrum (Figure 7B).

## Discussion

Ocular optics measurements from eyes of 31 healthy subjects who performed Vernier acuity and Landolt acuity threshold experiments were presented. Our main findings were:

1. Vernier acuity and Landolt acuity thresholds were significantly correlated across subjects, i.e., subjects who were good at discriminating Landolt optotypes were also good at detecting the offset in a pair of Vernier lines, and vice versa. Our data is among the largest singular sets on the relationship between these two acuity measurements in healthy subjects.
2. We found that subjects' Landolt acuity thresholds were significantly but weakly correlated with some

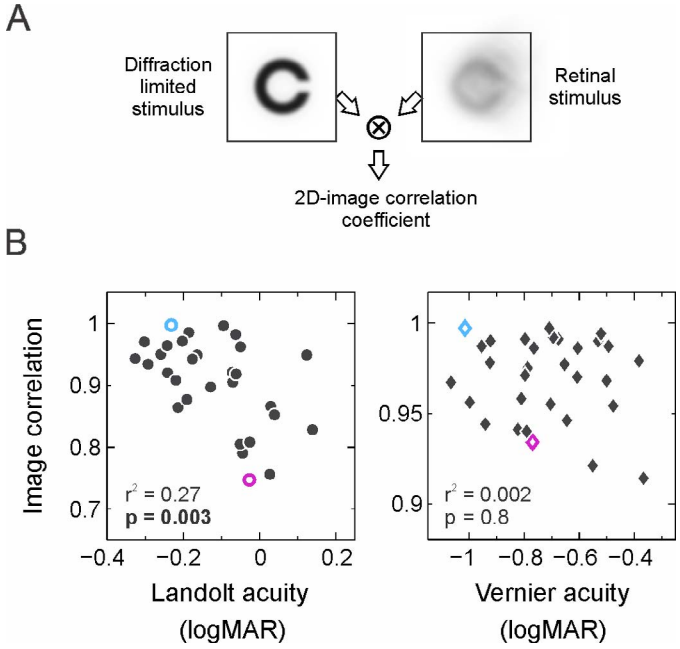


Figure 7. Stimulus-image correlation. (A) Schematic representation of the calculation of image correlation coefficients as a metric for retinal image quality. The two-dimensional image correlation coefficient is obtained by computing the cross-correlation for two stimuli, one convolved with the diffraction limited PSF, the other one convolved with the eye's individual PSF. (B) Stimulus image correlation coefficients are plotted as a function of Landolt (left)/Vernier (right) acuity thresholds ($n = 31$). Data points of the two subjects with the highest and lowest Strehl ratio are plotted in light blue and magenta, respectively (compare Figure 5). Only Landolt acuity correlates significantly with the image correlation coefficients, shown in the lower left corner of each plot.

higher order ocular optics metrics, both regarding the quality of the wavefront in the pupil plane, and regarding the quality of the retinal image. Subjects with more higher order ocular aberrations tended to have lower visual acuity. Albeit perhaps intuitive, this finding is not entirely trivial and is only partially supported by earlier studies.

3. Vernier acuity thresholds did not show a correlation with any of the optical quality metrics we tested. At the most extreme, some subjects exhibiting similar retinal images were both among the very best and the worst at discriminating the offset in the Vernier stimulus. Generally, no predictions about Vernier acuity could be drawn from optics measurements alone. To the best of our knowledge, this is the first report of Vernier acuity thresholds and their (missing) relationship to habitual optical quality.

There are only a few studies that directly compare perceptual performance in both hyperacuity and normal visual acuity tasks. Most of them investigate the relation between both types of acuity in visually deprived subjects. Significant correlations between Vernier and visual acuity were shown in amblyopic subjects with different etiologies of amblyopia and subjects with cataract. In the latter case, the slope of a linear fit to logarithmic Snellen and Vernier acuity was reported as 0.74 under optimal stimulus conditions (Enoch, Essock, & Williams, 1984). In amblyopia, slopes of subjects with strabismic and anisometropic etiology differed from the whole amblyopic population (slope = 1.15, $n = 427$). For anisometropes, the slope was 1.44, while for the strabismic subjects it was 0.79 (McKee, Levi, & Movshon, 2003). In an earlier study, the slopes in these groups were reversed, most likely explained by a much smaller sample size ($n = 12$) (Levi & Klein, 1982). In a group of normal controls ($n = 68$), significantly positive correlations were found between Vernier and visual acuity (McKee et al., 2003). A separate study analyzing differences between bisection discrimination and Vernier discrimination with and without visual backward masking did not find any correlation between visual acuity and Vernier acuity, and neither with other hyperacuity tasks (Cappe, Clarke, Mohr, & Herzog, 2014).

In our study, we find a significant but weak correlation between Landolt and Vernier acuity thresholds with a linear fit slope of 0.62 (Figure 2). Among obvious differences in methodology, one explanation of variation between our and earlier results might be eye selection. Throughout our analysis, we present data from the right eyes of all subjects only (to avoid bias), but we tested binocular and left eye performance as well. Although correlation coefficients and significance levels differ, left eye data ($n = 30$) show the same trends for the relation between acuity thresholds and the later discussed optical quality. Thus, our population possibly included preferred as well as nonpreferred eyes, a factor that might contribute to acuity correlations. For instance, data from McKee et al. (2003), which we reanalyzed by grouping into preferred and non-preferred eyes, showed differences among both groups: Landolt and Vernier acuity were only significantly correlated in preferred eyes (preferred: $r^2 = 0.14$, $p = 0.002$; nonpreferred: $r^2 = 0.03$, $p = 0.14$) (McKee et al., 2003). If we grouped our data into preferred (better Landolt acuity thresholds) and non-preferred eyes, we remain to find similar correlation trends in the preferred eye group, and no significant correlations for the non-preferred eyes, matching results from McKee et al. According to this grouping, our right eye data contained 61% preferred eyes (in which thresholds differed on average about 19% from the left eye), which supports the hypothesis that next to optical factors, neural mechanisms are playing a key role in the processing of acuity targets.

As a first summary, there seem to be factors in the visual pathway affecting both types of acuity and also factors that primarily influence only one of them. It may seem parsimonious to assume that external physical factors limiting acuity are also at play in hyperacuity tasks. It is clear that the eyes' optics influence retinal image formation, but the relationship between the ocular aberrations present in an individual eye and its performance in acuity tasks is more complex. By employing computationally aberrated letter charts it was shown that various optical metrics were significantly correlated with the decrease in acuity compared to nonaberrated letters (Marsack et al., 2004). Correspondingly, visual acuity of aberrated letters could be predicted from wavefront aberrations using different optically and physiologically informed models of spatial vision (Watson & Ahumada, 2008). Acuity was shown to be increasingly better in eyes with less aberrations when contrast and/or luminance is decreased (Applegate, Marsack, & Thibos, 2006). On the other hand, in subjects with normal and excellent visual acuity, no clear correlations between optical aberrations and low contrast tumbling E acuity could be found (Villegas et al., 2008). At high stimulus contrasts and short stimulus presentation times (to avoid potential temporal summation effects) the same study found weak correlations with single HOA components, i.e., coma, trefoil, and logarithmic Strehl ratio.

In our study, using more natural viewing conditions, we find a significant, if weak, correlation between Landolt acuity and the eye's individual HOA. We suggest that our study design, testing at smaller pupil sizes and in a subject group with more relaxed inclusion criteria, e.g., allowing for a wider range of visual acuities, might explain these differences. In any case, we also observe a wide distribution of visual acuity thresholds for similar amounts of aberrations, and this distribution of optical performance was even larger for Vernier acuity. Various factors may influence these variations in addition to the here investigated optical aberrations, such as cone photoreceptor density, ganglion cell density, intraocular scatter, neural adaptation, and cortical processing (Artal, 2015; Artal et al., 2004; Hou, Kim, & Verghese, 2017; Jiang et al., 2017; Rossi & Roorda, 2010; Wang et al., 2018).

Eye biometry data recorded here may act as an indirect measure of retinal sampling capacity. We found that axial length (AL) was positively correlated with Landolt acuity, but not with Vernier acuity. Axial elongation of the myopic eye, due to stretching of the retina, was found to be a primary cause for reduced sampling density of cone photoreceptors in the perifoveal region (Chui, Yap, Chan, & Thibos, 2005). Axial length (AL) was generally found to be highly negatively correlated to the sampling limit and packing density of the human cone mosaic (cones/mm$^2$) (Lombardo, Serrao, Ducoli, & Lombardo, 2012). A recent foveal cone density analysis obtained by adaptive optics scanning laser ophthalmoscopy in 28 healthy subjects confirmed a significant decrease in linear cone density (cones/mm$^2$) with increasing AL. However, considering that the foveal photoreceptor density might not decrease proportionally to the eye growth during myopic progression, the more appropriate unit for comparing AL and acuity would be the angular cone density (cones/deg$^2$). This analysis showed a significant increase of cones/deg$^2$ in longer eyes (Wang et al., 2018), suggesting a possible increase in visual acuity with increasing AL. However, another study, investigating the relationship between axial length and best corrected visual acuity, shows a significant decline in visual acuity for longer eyes (Lü et al., 2011), similarly to our results. In light of a possible increase in cone recruitment in myopic eyes, other factors might outweigh increased sampling. For habitual viewing, one factor might be a demagnified retinal image by spectacle correction. Additionally, eyeball elongation, which is highly correlated with increasing spherical equivalent, might introduce more HOA, which in turn decreases retinal image quality. This hypothesis is well studied and yet remains controversial. Various studies report significantly higher values for some of the HOA (Buehren, Collins, & Carney, 2005; Karimian, Feizi, & Doozande, 2010; Kasahara et al., 2017; Wei, Lim, Chan, & Tan, 2006) or total RMS (He et al., 2002; Marcos, Sawides, Gambra, & Dorronsoro, 2008; Paquin, Hamam, & Simonet, 2002) in higher myopic subjects. In contrast, Kwan et al. showed significantly smaller RMS values of fourth-order aberrations and spherical aberration in highly myopic than in nonmyopic eyes (Kwan, Yip, & Yap, 2009). Other studies reported that HOA were unrelated to refractive error (Cheng, Bradley, Hong, & Thibos, 2003) as well as AL (Lombardo et al., 2012), which can also be seen in our data (HOA vs AL, $r^2 = 0.01$, $p = 0.55$). Even if the relation between HOA and AL is still a matter of debate, both seem to be factors influencing visual acuity thresholds.

On a general note, a methodological limitation to our assessment of acuity was that subjects wore their habitual refractive correction during testing. This may have had an impact on data interpretation in different ways. First, optically, allowing for different correction devices resulted in retinal image size differences between eyes that were corrected with glasses and those corrected with contact lenses, due to additional demagnification in the case of glasses. However, since only three of the subjects with myopia higher than 1 D were wearing glasses for refractive correction, we do not expect a strong influence on the overall results. Second, we did not correct lower order aberrations

(LOA) beyond spectacle prescription during acuity testing. Therefore, any residual LOA could have affected performance during threshold measurements. However, residual LOA and acuity thresholds were not significantly correlated (Landolt: $r^2 = 0.24$, $p = 0.14$; Vernier: $r^2 = 0.04$, $p = 0.81$). Generally, a subjective refraction is highly fluctuating between different points in time, and the "best correction" was shown to vary about 0.25 to 0.5 D over a day (Chakraborty, Read, & Collins, 2014). LOA are therefore to be treated as a somewhat variable parameter. To account for this, we used optimized individual defocus values for each subject by letting them vary to maximize retinal image quality, as our visual system does naturally.

With regard to possible uncertainty of optics measurements in general, there are a few additional sources of variability to expect. For one, the iTrace aberrometer itself showed relatively good measurement repeatability for all Zernike coefficients (highest repeatability for corneal aberrations), but there is still some variation in the absolute amounts of individual Zernike coefficients, even for consecutive measured data (Visser et al., 2011). Also, there are small differences in measured aberrations across points in time (Srivannaboon, Reinstein, & Archer, 2007; Visser et al., 2011). HOA RMS fluctuations within one week or one year were shown to be on average 0.021 (week) and 0.031 (year) μm, respectively (Cheng, Himebaugh, Kollbaum, Thibos, & Bradley, 2004). Our mean HOA RMS across eyes was 0.22 μm. Thus, fluctuations of about 10% of our aberration values could be expected. Fluctuations of such amounts, however, are likely to not contribute much to image quality metrics, as they were shown to have almost no impact on the radial-averaged MTF, for instance (Cheng et al., 2004). We thus expect that the introduced variability of measurements of optical quality would not change our main finding. For following studies, it would be interesting to further investigate visual performance under the correction of individual lower and higher order aberrations, such as is provided in an adaptive optics stimulation system.

Because one of the goals of this study was to analyze the influence of aberrations under habitual viewing conditions, the procedure allowed for similar viewing conditions as the subjects had in everyday life, and thus visual degradation introduced by departure from aberrations that subjects were adapted to is minimized. It was shown that the neural visual system adapts to blur (Webster, Georgeson, & Webster, 2002) and to the eye's own aberrations (Artal et al., 2004). If subjects adapt to their specific aberration patterns, it may be reasonable to assume that the actual amount of aberrations would have a smaller effect on vision, a view that is supported by our general outcome that correlations between optics and acuity are significant but carry only a weak predictive power (all below 30% variability explained). Although the effect of neural adaptation is probably not too large, it may contribute to the robustness of the visual system, leading to similar performance for a large range of ocular optics quality in different subjects.

As a summary, we found clear differences between acuity and hyperacuity threshold in relation to the eye's optics, and it remains yet unclear which factors determine the distribution of Vernier thresholds in our subjects the most. That these individual differences might have real-world consequences can be derived from recent results looking at higher level perceptual tasks, such as reading. Vernier acuity potentially contributes to an early stage of hierarchical letter and word processing, as psychophysical thresholds in these tasks showed a correlation with the processing of Chinese characters (but not with other visual stimuli) (Tan et al., 2018). Moreover, visually evoked potentials (VEP) measured with Vernier targets allow for the characterization of the magnitude of acuity in amblyopic eyes better than VEP grating acuity (Hou et al., 2018).

Studies investigating the cortical sources of acuity go along with our findings. Functional testing of the visual cortex by electroencephalography showed that detection thresholds for grating acuity were similar in all four examined stages of cortical hierarchy [striate visual cortex (V1), hV4, lateral occipital cortex (LOC), middle temporal cortex], whereas only V1 and LOC were sensitive to Vernier displacements. This supports the hypothesis that grating acuity is limited by retinal sampling factors and that the striate cortex passes the information on to extrastriate cortices without further filtering. This may be different for Vernier acuity thresholds, as they show up in only two of the four examined cortical stages. The meaning of LOC for spatial perception processing is not completely understood yet, and it is discussed whether the activation of LOC might be related to a general sensitivity to the relative position of features (Hou et al., 2017). Conceptually, and supported by ideal-observer analysis, the retinal entry point to the visual path should also affect an observer's performance in hyperacuity tasks. The spatial information used to judge relative position in a foveal Vernier acuity task must be present in the spatial-temporal distribution of cone photoreceptor absorptions, because subsequent processing cannot add to this information. A biologically inspired simulation of the factors that potentially influence Vernier thresholds indicates eye movements, luminance level, defocus and bar length of the target as important factors (Jiang et al., 2017). Analyzing the exact spatiotemporal retinal sampling pattern during foveal inspection of a Vernier target and linking this directly to behavioral performance via photoreceptor-targeted

microstimulation (Harmening, Tuten, Roorda, & Sincich, 2014; Ratnam, Domdei, Harmening, & Roorda, 2017) could lend further insights into how far low-level retinal sampling behavior plays a role in hyperacute perception.

*Keywords: Vernier acuity*, *Landolt acuity*, *image blur*, *retinal sampling*, *psychophysics*, *aberrometry*, *spatial vision*

## Acknowledgments

The authors thank Frank Schaeffel for providing the pupillometry software. We thank all subjects for their patient participation in the experiments.

Supported by the National Institutes of Health (P30-EY001730), unrestricted grant from Research to Prevent Blindness (RS), and Emmy Noether Program of the German Research Foundation (DFG) Ha5323-5/1 (WMH). RS holds a career award at the Scientific Interfaces from the Burroughs Wellcome Fund and a career development award from the Research to Prevent Blindness.

At the time of data collection, ACL and WMH were affiliated with Institute of Zoology and Animal Physiology, RWTH Aachen, Germany.

Commercial relationships: none.
Corresponding author: Wolf M. Harmening.
Email: wolf.harmening@ukbonn.de.
Address: Department of Ophthalmology, University of Bonn, Germany.

## References

Abbud, C. M. M., & Cruz, A. A. V. (2002). Variability of Vernier acuity measurements in untrained subjects of different ages. *Brazilian Journal of Medical and Biological Research*, *35*(2), 223–227. retrieved from http://www.ncbi.nlm.nih.gov/pubmed/11847526

Applegate, R. A., Marsack, J. D., & Thibos, L. N. (2006). Metrics of retinal image quality predict visual performance in eyes with 20/17 or better visual acuity. *Optometry and Vision Science*, *83*(9), 635–640. https://doi.org/10.1097/01.opx.0000232842.60932.af

Artal, P. (2015). Image Formation in the Living Human Eye. *Annual Review of Vision Science*, *1*, 1–17. https://doi.org/10.1146/annurev-vision-082114-035905

Artal, P., Chen, L., Fernández, E. J., Singer, B., Manzanera, S., & Williams, D. R. (2004). Neural compensation for the eye's optical aberrations. *Journal of Vision*, *4*(4):4, 281–287, https://doi.org/10.1167/4.4.4. [PubMed] [Article]

Bach, M. (1996). The Freiburg Visual Acuity test–automatic measurement of visual acuity. *Optometry and Vision Science*, *73*(1), 49–53. Retrieved from http://www.ncbi.nlm.nih.gov/pubmed/8867682

Bach, M. (2007). The Freiburg Visual Acuity Test-variability unchanged by post-hoc re-analysis. *Graefe's Archive for Clinical and Experimental Ophthalmology*, *245*(7), 965–971. https://doi.org/10.1007/s00417-006-0474-4

Banton, T., & Levi, D. M. (1991). Binocular summation in vernier acuity. *Journal of the Optical Society of America A*, *8*(4), 673–680.

Bedell, H. E., Patel, S., & Chung, S. T. (1999). Comparison of letter and Vernier acuities with dioptric and diffusive blur. *Optometry and Vision Science*, *76*(2), 115–120. Retrieved from http://www.ncbi.nlm.nih.gov/pubmed/10082058

Bradley, A., & Skottun, B. C. (1987). Effects of contrast and spatial frequency on vernier acuity. *Vision Research*, *27*(10), 1817–1824.

Buehren, T., Collins, M. J., & Carney, L. G. (2005). Near work induced wavefront aberrations in myopia. *Vision Research*, *45*(10), 1297–1312. https://doi.org/10.1016/j.visres.2004.10.026

Bühren, J., Terzi, E., Bach, M., Wesemann, W., & Kohnen, T. (2006). Measuring contrast sensitivity under different lighting conditions: Comparison of three tests. *Optometry and Vision Science*, *83*(5), 290–298. https://doi.org/10.1097/01.opx.0000216100.93302.2d

Cappe, C., Clarke, A., Mohr, C., & Herzog, M. H. (2014). Is there a common factor for vision? *Journal of Vision*, *14*(8):4, 1–11, https://doi.org/10.1167/14.8.4. [PubMed] [Article]

Chakraborty, R., Read, S. A., & Collins, M. J. (2014). Diurnal variations in ocular aberrations of human eyes. *Current Eye Research*, *39*(3), 271–281. https://doi.org/10.3109/02713683.2013.841257

Cheng, X., Bradley, A., Hong, X., & Thibos, L. N. (2003). Relationship between refractive error and monochromatic aberrations of the eye. *Optometry and Vision Science*, *80*(1), 43–49. Retrieved from https://journals.lww.com/optvissci/Fulltext/2003/01000/Relationship_between_Refractive_Error_and.7.aspx

Cheng, X., Himebaugh, N. L., Kollbaum, P. S., Thibos, L. N., & Bradley, A. (2004). Test-retest reliability of clinical Shack-Hartmann measurements. *Investigative Ophthalmology and Visual Science*, *45*(1), 351–360. https://doi.org/10.1167/iovs.03-0265

Chui, T. Y. P., Yap, M. K. H., Chan, H. H. L., & Thibos, L. N. (2005). Retinal stretching limits peripheral visual acuity in myopia. *Vision Research*, *45*(5), 593–605. https://doi.org/10.1016/j.visres.2004.09.016

Curcio, C. A., Sloan, K. R., Kalina, R. E., & Hendrickson, A. E. (1990). Human photoreceptor topography. *The Journal of Comparative Neurology*, *292*(4), 497–523. https://doi.org/10.1002/cne.902920402

Enoch, J. M., Essock, E. A., & Williams, R. A. (1984). Relating vernier acuity and Snellen acuity in specific clinical populations. *Documenta Ophthalmologica*, *58*(1), 71–77.

Fahle, M. (1993). Visual learning in the hyperacuity range in adults. *German Journal of Ophthalmology*, *2*(2), 83–86.

Findlay, J. M. (1973, January 12). Feature detectors and vernier acuity. *Nature*, *241*(5385), 135–137.

Geisler, W. S. (1984). Physical limits of acuity and hyperacuity. *Journal of the Optical Society of America. A, Optics and Image Science*, *1*(7), 775–782. Retrieved from http://www.ncbi.nlm.nih.gov/pubmed/6747742

Harmening, W. M., Göbbels, K., & Wagner, H. (2007). Vernier acuity in barn owls. *Vision Research*, *47*(7), 1020–1026. https://doi.org/10.1016/j.visres.2007.01.005

Harmening, W. M., Tuten, W. S., Roorda, A., & Sincich, L. C. (2014). Mapping the perceptual grain of the human retina. *The Journal of Neuroscience*, *34*(16), 5667–5677. https://doi.org/10.1523/JNEUROSCI.5191-13.2014

He, J. C., Sun, P., Held, R., Thorn, F., Sun, X., & Gwiazda, J. E. (2002). Wavefront aberrations in eyes of emmetropic and moderately myopic school children and young adults. *Vision Research*, *42*(8), 1063–1070. https://doi.org/10.1016/S0042-6989(02)00035-4

Hering, E. (1899). Ueber die Grenzen der Sehschärfe [On the limits of visual acuity]. In *Berichte über die Verhandlungen der Königlich-Sächsischen Gesellschaft der Wissenschaften zu Leipzig. Mathematisch-Physische Classe; Naturwissenschaftlicher Teil*, *51* ( pp. 16–24). Leipzig, Germany: Georg Thieme.

Hirsch, J., & Curcio, C. A. (1989). The spatial resolution capacity of human foveal retina. *Vision Research*, *29*(9), 1095–1101.

Hou, C., Good, W. V., & Norcia, A. M. (2018). Detection of amblyopia using sweep VEP Vernier and grating acuity. *Investigative Ophthalmology & Visual Science*, *59*(3), 1435–1442. https://doi.org/10.1167/iovs.17-23021

Hou, C., Kim, Y.-J., & Verghese, P. (2017). Cortical sources of Vernier acuity in the human visual system: An EEG-source imaging study. *Journal of Vision*, *17*(6):2, 1–12, https://doi.org/10.1167/17.6.2. [PubMed] [Article]

Jiang, H., Cottaris, N., Golden, J., Brainard, D., Farrell, J. E., & Wandell, B. A. (2017). Simulating retinal encoding: Factors influencing Vernier acuity. *Electronic Imaging: Human Vision and Electronic Imaging*, *5*, 177–181.

Karimian, F., Feizi, S., & Doozande, A. (2010). Higher-order aberrations in myopic eyes. *Journal of Ophthalmic and Vision Research*, *5*(1), 3–9.

Kasahara, K., Maeda, N., Fujikado, T., Tomita, M., Moriyama, M., Fuchihata, M., & Ohno-Matsui, K. (2017). Characteristics of higher-order aberrations and anterior segment tomography in patients with pathologic myopia. *International Ophthalmology*, *37*(6), 1279–1288. https://doi.org/10.1007/s10792-016-0356-7

Kiorpes, L., Kiper, D. C., & Movshon, J. A. (1993). Contrast sensitivity and vernier acuity in amblyopic monkeys. *Vision Research*, *33*(16), 2301–2311. Retrieved from http://www.ncbi.nlm.nih.gov/pubmed/8273294

Krauskopf, J., & Farell, B. (1991). Vernier acuity: effects of chromatic content, blur and contrast. *Vision Research*, *31*(4), 735–749. Retrieved from http://www.ncbi.nlm.nih.gov/pubmed/1843773

Kwan, W. C. K., Yip, S. P., & Yap, M. K. H. (2009). Monochromatic aberrations of the human eye and myopia. *Clinical and Experimental Optometry*, *92*(3), 304–312. https://doi.org/10.1111/j.1444-0938.2009.00378.x

Levi, D. M., & Klein, S. A. (1982, July 15). Hyperacuity and amblyopia. *Nature*, *298*(5871), 268–270.

Levi, D. M., & Klein, S. A. (1990). Equivalent intrinsic blur in spatial vision. *Vision Research*, *30*(12), 1971–93. Retrieved from http://pesquisa.bvsalud.org/portal/resource/pt/mdl-2288101

Lieberman, H. R., & Pentland, A. P. (1982). Microcomputer-based estimation of psychophysical thresholds: The Best PEST. *Behavior Research Methods & Instrumentation*, *14*, 21–25.

Lindblom, B., & Westheimer, G. (1989). Binocular summation of hyperacuity tasks. *Journal of the Optical Society of America A*, *6*(4),585. https://doi.org/10.1364/JOSAA.6.000585

Lombardo, M., Serrao, S., Ducoli, P., & Lombardo, G. (2012). Variations in image optical quality of the eye and the sampling limit of resolution of the cone mosaic with axial length in young adults. *Journal of Cataract and Refractive Surgery*, *38*(7), 1147–1155. https://doi.org/10.1016/j.jcrs.2012.02.033

Lü, Y., Xia, W., Chu, R., Zhou, X., Dai, J., & Zhou, H. (2011). [Relationship between best corrected visual acuity and refraction parameters in myopia]. [In Chinese.] *Fa Yi Xue Za Zhi*, *27*(2), 94–97. Retrieved from http://www.ncbi.nlm.nih.gov/pubmed/21604445

Maeda, P. (2008). Zernike polynomials to generate non-spherical wavefront, diffraction, namely, transfer function. Retrieved from http://www.pudn.com/Download/item/id/472325.html

Marcos, S., Sawides, L., Gambra, E., & Dorronsoro, C. (2008). Influence of adaptive-optics ocular aberration correction on visual acuity at different luminances and contrast polarities. *Journal of Vision*, *8*(3):1, 1–12, https://doi.org/10.1167/8.13.1. [PubMed] [Article]

Marsack, J. D., Thibos, L. N., & Applegate, R. A. (2004). Metrics of optical quality derived from wave aberrations predict visual performance. *Journal of Vision*, *4*(4):8, 322–328, https://doi.org/10.1167/4.4.8. [PubMed] [Article]

McKee, S. P., Levi, D. M., & Movshon, J. A. (2003). The pattern of visual deficits in amblyopia. *Journal of Vision*, *3*(5),5. https://doi.org/10.1167/3.5.5

Mckee, S. P., & Westheimer, G. (1978). Improvement in vernier acuity with practice. *Perception & Psychophysics*, *24*, 258–262.

Murphy, K. M., & Mitchell, D. E. (1991). Vernier acuity of normal and visually deprived cats. *Vision Research*, *31*(2), 253–266.

Paquin, M., Hamam, H., & Simonet, P. (2002). Objective measurement of optical aberrations in myopic eyes. *Optometry and Vision Science*, *79*(5), 285–291. Retrieved from http://www.ncbi.nlm.nih.gov/pubmed/12035985

Ratnam, K., Domdei, N., Harmening, W. M., & Roorda, A. (2017). Benefits of retinal image motion at the limits of spatial vision. *Journal of Vision*, *17*(1):30, 1–11, https://doi.org/10.1167/17.1.30. [PubMed] [Article]

Ravikumar, S., Thibos, L. N., & Bradley, A. (2008). Calculation of retinal image quality for polychromatic light. *Journal of the Optical Society of America. A*, *25*(10), 2395–2407. https://doi.org/10.1364/JOSAA.25.002395

Rocha, K. M., Vabre, L., Chateau, N., & Krueger, R. R. (2010). Enhanced visual acuity and image perception following correction of highly aberrated eyes using an adaptive optics visual simulator. *Journal of Refractive Surgery*, *26*(1), 52–56. https://doi.org/10.3928/1081597X-20101215-08

Rossi, E. A., & Roorda, A. (2010). The relationship between visual resolution and cone spacing in the human fovea. *Nat Neurosci*, *13*(2), 156–157. https://doi.org/10.1038/nn.2465

Schwiegerling, J. (2002). Scaling Zernike expansion coefficients to different pupil sizes. *Journal of the Optical Society of America A: Optics, Image Science, and Vision*, *19*(10), 1937–1945.

Seymoure, P., & Juraska, J. M. (1997). Vernier and grating acuity in adult hooded rats: The influence of sex. *Behavioral Neuroscience*, *111*(4), 792–800. Retrieved from http://www.ncbi.nlm.nih.gov/pubmed/9267656

Srivannaboon, S., Reinstein, D. Z., & Archer, T. J. (2007). Diurnal variation of higher order aberrations in human eyes. *Journal of Refractive Surgery*, *23*(5), 442–446. https://doi.org/10.1016/j.jalz.2013.05.1020

Strasburger, H., Huber, J., & Rose, D. (2018). Ewald Hering's (1899) on the limits of visual acuity: A translation and commentary - With a supplement on Alfred Volkmann's (1863) Physiological Investigations in the Field of Optics. *I-Perception*, *9*(3) (1899), 1–14. https://doi.org/10.1177/2041669518763675

Tan, Y., Tong, X., Chen, W., Weng, X., He, S., & Zhao, J. (2018). Vernier but not grating acuity contributes to an early stage of visual word processing. *Neuroscience Bulletin*, *34*(3), 517–526. https://doi.org/10.1007/s12264-018-0220-z

Thibos, L. N., Hong, X., Bradley, A., & Applegate, R. A. (2004). Accuracy and precision of objective refraction from wavefront aberrations. *Journal of Vision*, *4*(4):9, 329–351, https://doi.org/10.1167/4.4.9. [PubMed] [Article]

Thibos, L. N., Hong, X., Bradley, A., & Cheng, X. (2002). Statistical variation of aberration structure and image quality in a normal population of healthy eyes. *Journal of the Optical Society of America. A, Optics, Image Science, and Vision*, *19*(12), 2329–2348. https://doi.org/10.1364/JOSAA.19.002329

Thibos, L. N., Wheeler, W., & Horner, D. (1997). Power vectors: An application of Fourier analysis to the description and statistical analysis of

refractive error. *Optometry and Vision Science*, *74*(6), 367–375. Retrieved from http://www.ncbi.nlm.nih.gov/pubmed/9255814

Villegas, E. A., Alcon, E., & Artal, P. (2008). Optical quality of the eye in subjects with normal and excellent visual acuity. *Investigative Ophthalmology and Visual Science*, *49*(10), 4688–4696. https://doi.org/10.1167/iovs.08-2316

Visser, N., Berendschot, T. T. J. M., Verbakel, F., Tan, A. N., de Brabander, J., & Nuijts, R. M. M. A. (2011). Evaluation of the comparability and repeatability of four wavefront aberrometers. *Investigative Ophthalmology and Visual Science*, *52*(3), 1302–1311. https://doi.org/10.1167/iovs.10-5841

Wang, Y., Bensaid, N., Tiruveedhula, P., Ma, J., Roorda, A., & Ravikumar, S. (2018). The relationship between cone density and axial length: CAL study. In *Annual Meeting of the Association for Research in Vision and Ophthalmology (ARVO)*. Berkeley, California, United States.

Watson, A. B., & Ahumada, A. J. (2008). Predicting visual acuity from wavefront aberrations. *Journal of Vision*, *8*(4):17, 1–19, https://doi.org/10.1167/8.4.17. [PubMed] [Article]

Webster, M. A., Georgeson, M. A., & Webster, S. M. (2002). Neural adjustments to image blur. *Nature Neuroscience*, *5*(9), 839–840. https://doi.org/10.1038/nn906

Wehrhahn, C., & Westheimer, G. (1990). How vernier acuity depends on contrast. *Experimental Brain Research*, *80*(3), 618–620. Retrieved from http://www.ncbi.nlm.nih.gov/pubmed/2387359

Wei, R. H., Lim, L., Chan, W. K., & Tan, D. T. H. (2006). Higher order ocular aberrations in eyes with myopia in a Chinese population. *Journal of Refractive Surgery*, *22*(7), 695–702. Retrieved from http://www.ncbi.nlm.nih.gov/pubmed/16995552

Westheimer, G. (1975). Visual acuity and hyperacuity. *Investigative Ophthalmology*, *64*(8), 570–572. https://doi.org/10.1097/00006324-198708000-00002

Westheimer, G. (2009). Visual acuity: Information theory, retinal image structure and resolution thresholds. *Progress in Retinal and Eye Research*, *28*(3), 178–186. https://doi.org/10.1016/j.preteyeres.2009.04.001

Westheimer, G., & McKee, S. P. (1975). Visual acuity in the presence of retinal-image motion. *Journal of the Optical Society of America*, *65*(7), 847–850. Retrieved from http://www.ncbi.nlm.nih.gov/pubmed/1142031

Westheimer, G., & McKee, S. P. (1977). Spatial configurations for visual hyperacuity. *Vision Research*, *17*(8), 941–947. Retrieved from http://www.ncbi.nlm.nih.gov/pubmed/595400

Westheimer, G., Shimamura, K., & McKee, S. P. (1976). Interference with line-orientation sensitivity. *Journal of the Optical Society of America*, *66*(4), 332–338. Retrieved from http://www.ncbi.nlm.nih.gov/pubmed/1262981

Whitaker, D., & MacVeigh, D. (1991). Interaction of spatial frequency and separation in vernier acuity. *Vision Research*, *31*(7–8), 1205–1212.

Williams, R. A., Enoch, J. M., & Essock, E. A. (1984). The resistance of selected hyperacuity configurations to retinal image degradation. *Investigative Ophthalmology & Visual Science*, *25*(4), 389–399.

Wülfing, E. A. (1892). Ueber den kleinsten Gesichtswinkel. *Zeitschrift Für Biologie*, *29*, 199–202.

Yoon, G., & Williams, D. R. (2002). Visual performance after correcting the monochromatic and chromatic aberrations of the eye. *Journal of the Optical Society of America A*, *19*(2), 266–275.

Zheleznyak, L., Sabesan, R., Oh, J. S., MacRae, S., & Yoon, G. (2013). Modified monovision with spherical aberration to improve presbyopic through-focus visual performance. *Investigative Ophthalmology and Visual Science*, *54*(5), 3157–3165. https://doi.org/10.1167/iovs.12-11050